JOURNAL OF VIROLOGY, Dec. 2010, p. 12385–12396 Vol. 84, No. 23
0022-538X/10/$12.00 doi:10.1128/JVI.01229-10
Copyright © 2010, American Society for Microbiology. All Rights Reserved.

Role of Erythropoietin Receptor Signaling in Parvovirus B19 Replication in Human Erythroid Progenitor Cells▽

Aaron Yun Chen,[1]# Wuxiang Guan,[1]# Sai Lou,[1,2] Zhengwen Liu,[2] Steve Kleiboeker,[3] and Jianming Qiu[1]*

Department of Microbiology, Molecular Genetics and Immunology, University of Kansas Medical Center, Kansas City, Kansas[1]; Department of Infectious Diseases, The First Affiliated Hospital, Xi'an Jiaotong University, Xi'an, China[2]; and ViraCor Laboratories, Lee's Summit, Missouri[3]

Received 8 June 2010/Accepted 14 September 2010

Parvovirus B19 (B19V) infection is highly restricted to human erythroid progenitor cells. Although previous studies have led to the theory that the basis of this tropism is receptor expression, this has been questioned by more recent observation. In the study reported here, we have investigated the basis of this tropism, and a potential role of erythropoietin (Epo) signaling, in erythroid progenitor cells (EPCs) expanded *ex vivo* from CD34$^+$ hematopoietic cells in the absence of Epo (CD36$^+$/Epo$^-$ EPCs). We show, first, that CD36$^+$/Epo$^-$ EPCs do not support B19V replication, in spite of B19V entry, but Epo exposure either prior to infection or after virus entry enabled active B19V replication. Second, when Janus kinase 2 (Jak2) phosphorylation was inhibited using the inhibitor AG490, phosphorylation of the Epo receptor (EpoR) was also inhibited, and B19V replication in *ex vivo*-expanded erythroid progenitor cells exposed to Epo (CD36$^+$/Epo$^+$ EPCs) was abolished. Third, expression of constitutively active EpoR in CD36$^+$/Epo$^-$ EPCs led to efficient B19V replication. Finally, B19V replication in CD36$^+$/Epo$^+$ EPCs required Epo, and the replication response was dose dependent. Our findings demonstrate that EpoR signaling is absolutely required for B19V replication in *ex vivo*-expanded erythroid progenitor cells after initial virus entry and at least partly accounts for the remarkable tropism of B19V infection for human erythroid progenitors.

Parvovirus B19 (B19V) is pathogenic to humans. It replicates autonomously and belongs to the genus *Erythrovirus* in the family *Parvoviridae* (14). Clinical manifestations of B19V infection vary among different health conditions. The most common manifestation is erythema infectiosum. However, B19V infection often results in bone marrow failure under the following conditions (9, 10, 62). In patients with increased destruction of erythrocytes and a high turnover of erythrocytes (e.g., sickle cell disease patients), acute B19V infection can cause transient aplastic crisis. In immunocompromised patients, persistent B19V infection may develop manifestations as pure red-cell aplasia, a chronic anemia. Moreover, B19V fetal infection can cause severe anemia in the fetus, resulting in nonimmune hydrops fetalis and fetal death (1, 2, 16, 47, 57).

Erythropoiesis is the process whereby a fraction of primitive multipotent hematopoietic stem cells (CD34$^+$) commit to the erythroid lineage, forming burst-forming units-erythroid (BFU-E; earlier erythroid progenitor) cells, CFU-erythroid (CFU-E; later erythroid progenitor) cells, normoblasts, erythroblasts, reticulocytes, and ultimately, mature erythrocytes. B19V infection shows a remarkable tropism for BFU-E and CFU-E progenitors in human bone marrow and fetal livers. Notably, both cell types express the cell surface marker CD36 (30, 39, 50, 60). The clinical manifestations of B19V infection seen in both aplastic crisis and pure red-cell aplasia are direct outcomes of cell death of the erythroid progenitors that are targets of B19V replication, and this cell death is due to direct cytotoxicity of the virus infection (9, 13). Progressive host cell apoptosis has been observed during B19V infection of erythroid progenitor cells (29, 49, 60), and this is likely induced during infection of the abundantly expressed 11-kDa nonstructural protein of the virus (12). Apoptosis of erythroid progenitor cells is also characteristic of B19V-induced hydrops fetalis (60).

Polyadenylation at the proximal site [(pA)p], which is located in the center of the B19V genome, precludes the inclusion of the capsid-encoding open reading frame (ORF) in transcripts under some conditions (38, 61). We have recently shown that replication of the B19V genome enhances readthrough of the (pA)p and, thereafter, the polyadenylation of B19V transcripts at the distal site. Therefore, replication of the B19V genome facilitates the production of a sufficient number of full-length transcripts encoding the viral capsid proteins to achieve productive infection (21). The remarkable tropism of B19V for human erythroid progenitors was initially believed to be due to cell type-specific expression of the blood group P antigen (globoside), which serves as the cellular receptor for B19V (8). However, recent findings revealed an additional requirement for the coreceptors integrin α5β1 (55) and KU80 (32); i.e., erythrocyte P antigen is necessary, but not sufficient, for B19V binding and entry into the cell (54).

More about the B19V tropism has been learned from the fact that in addition to the native target cells for B19V infection in human bone marrow and fetal livers, a few cell lines (the megakaryoblastoid cell line UT7/Epo-S1 [31] and the erythroid leukemic cell line KU812Ep6 [28]) support B19V rep-

* Corresponding author. Mailing address: Department of Microbiology, Molecular Genetics and Immunology, Mail Stop 3029, 3901 Rainbow Blvd., Kansas City, KS 66160. Phone: (913) 588-4329. Fax: (913) 588-7295. E-mail: jqiu@kumc.edu.
# These authors contributed equally.
▽ Published ahead of print on 22 September 2010.

TABLE 1. Media used for $CD36^+$ EPC expansion[a]

Medium	Serum-free base	Amt of cytokine in medium					
		SCF	IL-6	IL-3	Flt-3-L	TPO	Epo
StemCell	SFEM	100 ng/ml	20 ng/ml	20 ng/ml	20 ng/ml	50 ng/ml	None
Wong	BIT in AMEM	100 ng/ml	None	5 ng/ml	None	None	3 U/ml

[a] Serum-free expansion medium (SFEM) and BIT 9500 (BIT) were obtained from StemCell Technologies, Inc. (Vancouver, British Columbia, Canada). With the exception of Epo, which was obtained from Amgen, all cytokines were purchased from Invitrogen. SCF, stem cell factor; IL-6, interleukin-6; IL-3, interleukin-3; Flt-3-L, Flt-3 ligand; TPO, thrombopoietin. In addition to the components listed, Wong medium also contains 900 ng/ml of Fe^{2+}, 90 ng/ml of Fe^{3+}, and 1 μM hydrocortisone, as described previously (21, 56).

lication, albeit at a limited efficiency (7, 56). Recently, *ex vivo*-expanded $CD36^+$ erythroid progenitor cells ($CD36^+$ EPCs) have proven to be highly permissive to B19V infection and to support active B19V replication (≥100-fold increase in the B19V genome copy number) (19, 21, 43, 49, 56). All B19V-semipermissive cell lines and primary $CD36^+$ EPCs require erythropoietin (Epo) to sustain proliferation, suggesting that Epo is required for B19V infection. Epo has been confirmed to be essential for the susceptibility of human bone marrow cells to B19V infection (52), and based on this, it was concluded that the B19V target cells are of the erythroid lineage, including BFU-E progenitors through erythroblasts, with the susceptibility to B19V infection increasing with maturity (52). Thus, the main role of Epo in B19V permissiveness was thought to be differentiation of bone marrow hematopoietic stem cells (HSCs) into the stage of erythroid progenitors.

In this study, we show that Epo, specifically the Epo/Epo receptor (EpoR)/Janus kinase 2 (Jak2) pathway, plays a direct role in supporting replication of the B19V genome. We prepared $CD36^+$ EPCs by *ex vivo* expanding $CD34^+$ HSCs in the absence of Epo (Epo^-) or presence of Epo (Epo^+). $CD36^+$ EPCs expanded in StemCell medium (no Epo) (Table 1), namely, $CD36^+/Epo^-$ EPCs, were not permissive to B19V infection, although virus did enter the cells. However, when Epo was added either prior to or after virus infection, $CD36^+/Epo^-$ EPCs became permissive to B19V replication. Moreover, inhibition of EpoR signaling, by applying either the Jak2-specific inhibitor AG490 or a Jak2-specific short hairpin RNA (shRNA), reduced B19V replication in $CD36^+$ EPCs expanded in Wong medium (with Epo; $CD36^+/Epo^+$ EPCs) (Table 1). Expression of constitutively active EpoR in $CD36^+/Epo^-$ EPCs led to an increase in B19V replication, bringing it to a level comparable to that observed in $CD36^+/Epo^+$ EPCs. Thus, our study brings to light a novel indispensable role of the Epo/EpoR/Jak2 pathway in B19V replication, which partially accounts for the fact that B19V propagates only in cells that require Epo for their proliferation.

MATERIALS AND METHODS

Generation of $CD36^+$ EPCs. $CD34^+$ HSCs were purchased from the National Disease Research Interchange (NDRI), Philadelphia, PA.

For the generation of $CD36^+/Epo^+$ EPCs, $CD34^+$ HSCs were *ex vivo* expanded in Wong medium (Table 1) upon arrival of the cells (day 0) and stored in liquid nitrogen on day 4, as described previously (21, 56). Once the day 4 stock cells were thawed, they were cultured in Wong medium for an additional 4 days before being used in experiments.

StemCell medium was prepared from StemSpan serum-free expansion medium (SFEM; StemCell Technologies Inc., Vancouver, British Columbia, Canada) and a combination of cytokines (Table 1). $CD34^+$ HSCs were *ex vivo* expanded in StemCell medium from day 0 continuously until day 8. These cells were used only for experiments described in the legend to Fig. 1.

For the generation of $CD36^+/Epo^-$ EPCs, 3×10^6 $CD34^+$ HSCs were cultured in StemCell medium. At day 6 or 8, approximately 2×10^7 to 3×10^7 expanded cells were spun down at $300 \times g$ for 10 min, resuspended in 1 ml of autoMACS rinsing buffer (Miltenyi Biotec, Auburn, CA), and incubated with mouse anti-human CD36 antibody (10^6 cells/μl; BD Biosciences) for 15 min at 4°C. Then cells were spun down at 2,250 rpm for 2 min and washed three times with the autoMACS rinsing buffer. After incubation with anti-mouse IgM-coated magnetic microbeads (Miltenyi Biotec) for 15 min at 4°C, cells were loaded onto a MiniMACS column, and the labeled cells were eluted by following the manufacturer's instructions.

Construction and production of retroviral and lentiviral vectors. (i) Retroviral vectors expressing EpoR(R129C). Plasmid pMSCV-EpoR(R129C)-IRES-GFP was constructed by inserting the EpoR(R129C) gene (20) into the BamHI-XbaI-digested pMSCV-MCS-IRES-GFP-WPRE vector. Retroviruses (Retro-EpoR and Retro-green fluorescent protein [GFP]) were produced by transfecting pMSCV-EpoR(R129C)-IRES-GFP and pMSCV-IRES-GFP with pCMV-VSVG in GP293 cells (Clontech). Concentration of retroviral vectors was carried out by following the manufacturer's instructions (catalog no. PT3132-1; Clontech).

(ii) Lentiviral vectors expressing shRNAs. We obtained the pLKO.1 cloning vector and the pLKO-Scramble-shRNA vector from Addgene Inc. (Cambridge, MA). The puromycin resistance gene in the pLKO vectors was replaced with the GFP ORF from pC1GFP (Clontech), using the BamHI/KpnI sites, generating pLKO-GFP and pLKO-GFP-Scramble-shRNA, respectively. The validated JAK2 shRNA1 sequence (TRCN0000003181; Sigma) (GenBank accession no. NM_004972) was cloned into pLKO-GFP using the AgeI and EcoRI sites, generating pLKO-GFP-Jak2-shRNA. Lentivirus was generated and concentrated by following Addgene's instructions (http://www.addgene.org/plko).

Virus and infection. We obtained B19V viremic plasma samples, P20 (21) and P32, from ViraCor Laboratories (Lee's Summit, MO) and quantified the number of B19V genomic copies (gc) for each (10^{12} gc/ml), as previously described (21). Infection was performed at a multiplicity of infection (MOI) of 1 fluorescent focus-forming unit (FFU) per cell (approximately 5,000 gc/cell). Except for the experiments illustrated in Fig. 1, in which plasma sample P20 was used, all other experiments were carried out using P32 for the sake of consistency. B19V infection of $CD36^+$ EPCs expanded in both samples was carried out at culture day 8.

For lentiviral and retroviral transduction, concentrated lentiviral retrovirus was added to $CD36^+$ EPCs at day 6 of culture at an MOI of 4 FFU/cell. B19V infection was carried out at 48 h posttransduction (p.t.).

Viral entry and replication quantification assays. We performed a viral entry assay as previously described (3). Briefly, cells were infected with B19V at an MOI of 1. After 2 h of incubation with the virus, the cells were washed with AMEM (alpha modification of Eagle's medium; Mediatech, Manassas, VA), and spun down at 2,200 rpm for 3 min. The cell pellet was then resuspended at 0.5 million cells per 100 μl of trypsin-EDTA (0.25% trypsin in 20 mM EDTA buffer) for 5 min at 37°C. Total DNA was extracted using the blood DNA minikit (Qiagen), according to the manufacturer's instructions. The number of B19V genome copies in the extracted DNA was then assayed by quantitative real-time PCR (qPCR) as described previously (22). The replicated viral DNA was extracted as described above and quantified by qPCR at 48 h postinfection (p.i.), except in the case of experiments carried out at 24 h p.i. (see Fig. 5).

Southern blot analysis. At 48 h p.i., cells were harvested for Hirt DNA extraction, and Hirt DNA samples were analyzed by Southern blotting as described previously (21, 22). Blots were exposed to a GE phosphor imaging screen and quantified using a phosphor imager (Storm 856) and ImageQuant TL software, version 2005 (GE Healthcare).

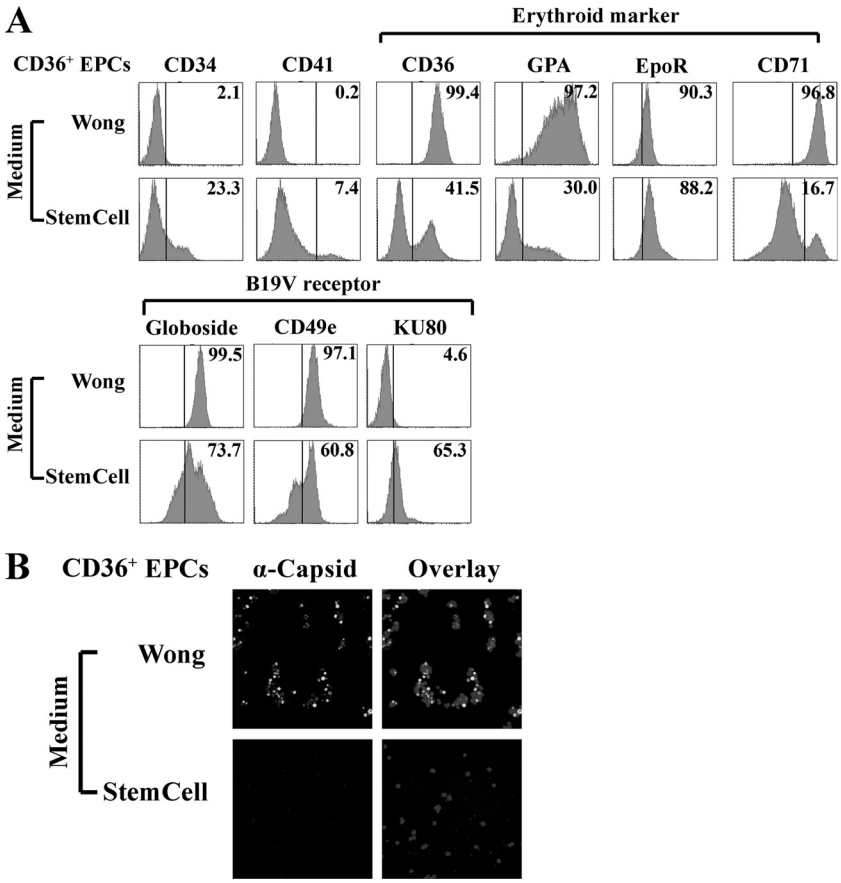

FIG. 1. CD36$^+$ EPCs expanded in StemCell medium lacking Epo are not permissive to B19V infection. CD34$^+$ HSCs were cultured in StemCell or Wong medium (Table 1, formulation). (A) At day 8 of culture, expression of the indicated surface markers on cells from different cultures was analyzed. For surface staining, antibodies against the cell surface antigens CD34, CD36, CD41, GPA, CD71, and CD49e (all obtained from BD Biosciences, San Jose, CA), as well as those against the surface-localized receptors globoside (Matreya, Pleasant Gap, PA), KU80 (Calbiochem, San Diego, CA), and EpoR (Abcam, Cambridge, MA), were used to characterize cell phenotype. Numbers in each panel indicate the percentage of positive cells among the population. A representative result from two independent experiments is shown. (B) At day 8 of culture, B19V infection was carried out as described in Materials and Methods. Immunofluorescence staining was performed at 48 h p.i., using antibody against the B19V capsid. DAPI was used to stain the nuclei. Images were acquired at 40× magnification, using an Eclipse C1 Plus confocal microscope (Nikon).

Reverse transcription (RT) and RT-qPCR. We extracted mRNA using a TurboCapture mRNA kit (Qiagen) by following the manufacturer's instructions. We then performed reverse transcription directly in the TurboCapture tubes, using random hexamers (Promega) and Moloney murine leukemia virus (MMLV) RT (Invitrogen). A multiplex RT-qPCR was performed to detect B19V VP2-encoding mRNA and the B19V mRNAs spliced from the D1 donor site to the A1-2 acceptor site (D1/A1-2-spliced mRNA) (21), with β-actin mRNA serving as an internal control, as previously reported (21, 22).

Immunofluorescence. Infected cells were cytocentrifuged at 1,500 rpm for 5 min and fixed in a mixture of acetone and methanol (1:1 dilution) at −20°C for 15 min. The staining was performed as previously described using anti-B19V capsid (clone 521-5D) and fluorescein isothiocyanate (FITC)-conjugated anti-mouse IgG (22).

Western blot analysis. Cell lysates were prepared at 48 h posttreatment and used for Western blot analysis as previously described (46).

Cell viability assay. We examined cell viability using the CellTiter-Glo kit (Promega), which determines the number of viable cells in culture based on quantification of the ATP presence in cells by following the manufacturer's instructions.

Flow cytometry analysis. For cell surface staining, 10^5 cells were incubated with the first antibody at a 1:100 dilution in a volume of 100 μl of phosphate-buffered saline (PBS) containing 2% fetal calf serum (FCS) for 30 min at room temperature. After being washed twice with PBS-FCS, the cells were incubated with FITC-conjugated secondary antibody at a dilution of 1:100 for 30 min at room temperature. After being washed, the cells were fixed in 1% paraformaldehyde.

For intracellular staining, annexin V/propidium iodide (PI) and DAPI (4′,6-diamidino-2-phenylindole) staining were performed essentially as described previously (11).

RESULTS

CD36$^+$ EPCs differentiated from CD34$^+$ HSCs in the absence of Epo are not permissive to B19V infection. To distinguish between potential roles for Epo in differentiating human HSCs and in supporting B19V replication, we generated erythroid progenitor cells that possess the erythroid progenitor marker CD36 (17, 37). This was accomplished by stimulating the differentiation of human bone marrow derived-HSCs (CD34$^+$) in two expansion media, Wong medium (with Epo) and StemCell medium (without Epo), which contain different combinations of cytokines, as described in Table 1.

At day 8 in culture, cells grown in the two media were analyzed by flow cytometry with antibodies to a panel of ery-

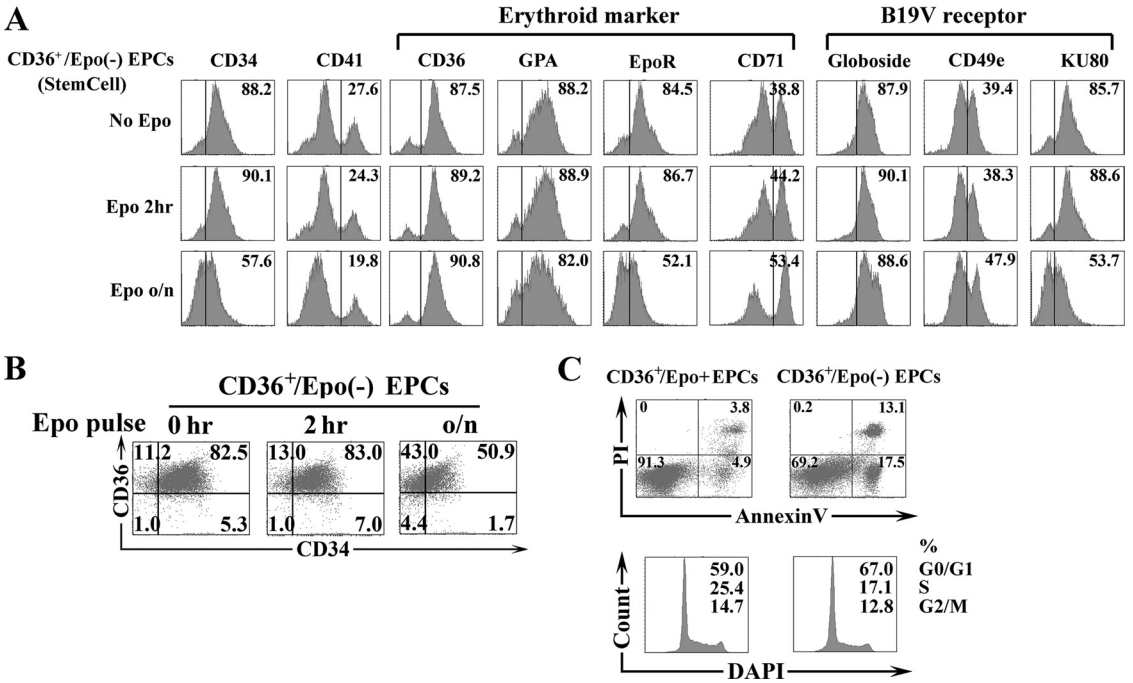

FIG. 2. An Epo pulse stimulates differentiation of $CD36^+/Epo^-$ EPCs toward $CD36^+/Epo^+$ EPCs. Purified $CD36^+/Epo^-$ EPCs were pulsed with Epo (3 U/ml) for different lengths of time and were analyzed after 8 days in culture. $CD36^+/Epo^+$ EPCs expanded in Wong medium were used as controls. (A) Expression of the indicated surface markers. (B) Expression of CD34 and CD36. (C) Annexin V/PI staining for assessment of cell death and DAPI staining for cell cycle analysis. For annexin V/PI staining, the numbers shown in the lower left quadrants represent the percentages of live cells, and the numbers in the upper and lower right quadrants represent the percentages of later and early stage apoptotic cells, respectively. In the case of DAPI staining, the three sets of numbers represent the percentages of cells in each phase of the cell cycle (G_0/G_1, S, and G_2/M). o/n, overnight.

throid markers (CD36, glycophorin A [GPA], EpoR, and CD71), the B19V receptor (Globoside) (8) and its coreceptors (CD49e and KU80), (32, 55), and the CD41 megakaryoblastic marker (53), as well as CD34 of the HSC lineage. Of the cells that were *ex vivo* expanded in Wong medium and StemCell medium, 99.4% and 41.5% expressed CD36, respectively (Fig. 1A). Cells expanded in StemCell medium retained a considerable level of CD34 (23.3%), and a low level of CD41 (7.4%) (Fig. 1A), indicating that they had differentiated toward an erythroid progenitor fate. CD71, the transferrin receptor, was expressed at 96.8% and 16.7% on cells expanded in Wong and StemCell media, respectively (Fig. 1A). Expression of GPA was significantly enhanced (97.2%) on the $CD36^+$ EPCs expanded in Wong medium, whereas only 30.0% on the cells expanded in StemCell medium (Fig. 1A). Cells expanded in both media expressed high levels of globoside, CD49e, the primary receptor and coreceptor for B19V infection (8, 32, 55), and EpoR (Fig. 1A). Interestingly, KU80, which has been proposed to serve as a coreceptor for B19V (32), was expressed on approximately 65.3% of the cells expanded in StemCell medium but on only 4.6% of the cells expanded in Wong medium (Fig. 1A).

We then infected the two types of $CD36^+$ EPCs with B19V in their respective media for 2 days. B19V infectivity was then examined by immunofluorescence staining with an anti-B19V capsid antibody (Fig. 1B). Unexpectedly, $CD36^+$ EPCs expanded in StemCell medium (no Epo) were not permissive to B19V infection, as shown by a lack of anti-capsid staining. Conversely, in $CD36^+$ EPCs expanded in Wong medium (with Epo at 3 units/ml), more than 80% of the cells were positive for capsid detection, indicating that infection was effective (56). This result suggests that the committed erythroid progenitor cells cultured in the absence of Epo are not permissive to B19V infection and that Epo not only is required for the differentiation of erythroid progenitor cells but also may be necessary for B19V infection of erythroid progenitor cells.

Epo-dependent B19V infection of $CD36^+/Epo^-$ EPCs leads to replication of the viral genome. We next purified $CD36^+$ EPCs from the cells expanded in StemCell medium. The purified cells, referred as $CD36^+/Epo^-$ EPCs, were analyzed by flow cytometry and uniformly found to express markers of erythroid progenitors (i.e., $CD36^+$ at 87.5%, GPA^+ at 88.2%, and $EpoR^+$ at 84.5%) and high levels of the B19V receptor ($globoside^+$ at 87.9%) and its coreceptors ($CD49e^+$ at 39.4% and $KU80^+$ at 85.7%). Interestingly, most of these purified cells (82.5%) expressed both CD34 and CD36 (Fig. 2B, 0 h), indicating that they represented BFU-E cells or cells in transition from the BFU-E to the CFU-E stage (37). StemSpan SFEM (the base medium used here) supplemented with cytokines has been widely used for the culture and expansion of human HSCs. To ensure that $CD34^+$ HSC expansion toward $CD36^+$ EPCs was optimal and to guarantee that the purified $CD36^+$ EPCs entered S phase to complete cell division, even in the absence of Epo, we used the following cytokine combination: stem cell factor (SCF), Flt-3, interleukin-3 (IL-3), IL-6, and thrombopoietin (TPO) (technical bulletin no. 29954;

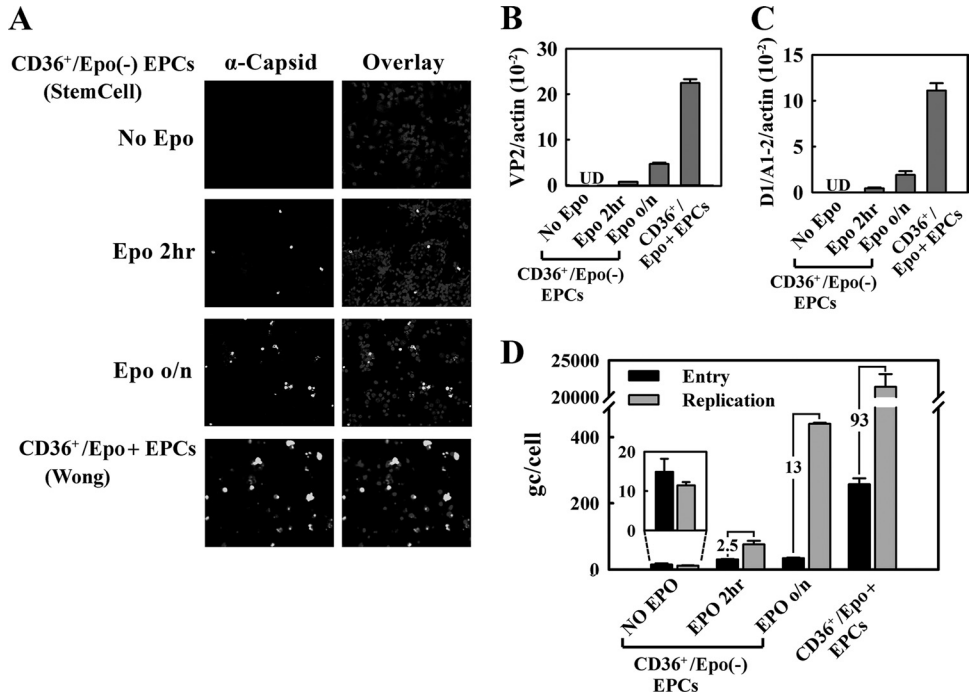

FIG. 3. An Epo pulse stimulates expression of the B19V capsid in CD36$^+$/Epo$^-$ EPCs. CD36$^+$/Epo$^-$ EPCs were pulsed with Epo (3 U/ml) for different lengths of time prior to B19V infection. CD36$^+$/Epo$^+$ EPCs expanded in Wong medium were used as controls. Analysis was performed at 48 h p.i. (A) Immunofluorescence staining for the B19V capsid, with DAPI costaining revealing the nucleus. Images were acquired at a magnification of ×40, using an Eclipse C1 Plus confocal microscope (Nikon). (B and C) Multiplex RT-qPCR-based quantification of VP2-encoding (B) and D1/A1-2-spliced (C) mRNAs. Values shown are the average numbers of mRNA copies per β-actin mRNA (internal control), with standard deviation indicated. UD, undetectable. (D) B19V entry and DNA replication, assessed as described in Materials and Methods. The numbers in the panel indicate the fold differences between replication and entry. Bars for the "no Epo" group are enlarged for better comparison.

StemCell Technologies Inc.) (Table 1) (63, 64). As shown in Fig. 2C, most of the purified CD36$^+$/Epo$^-$ EPCs (approximately 70%) survived through day 8 of culture in the absence of Epo, and these surviving cells entered S phase at a rate of 17%. This result indicates that the combination of cytokines in the StemCell medium enabled the survival of the CD36$^+$/Epo$^-$ EPCs in the absence of Epo and that it is suitable for parvovirus B19V infection experiments. Similar to unpurified cells expanded in StemCell medium (Fig. 1B), purified CD36$^+$/Epo$^-$ EPCs were not susceptible to B19V infection, as revealed by a lack of detectable capsids and B19V mRNAs (Fig. 3A to C).

To examine whether Epo is required for B19V infection, we pretreated purified CD36$^+$/Epo$^-$ EPCs with Epo (3 units/ml) for 2 h or overnight (approximately 16 h) prior to B19V infection. Interestingly, cells treated with Epo for either lengths of time became susceptible to B19V infection to some extent (Fig. 3A to C). Following overnight Epo treatment, approximately 10% of the purified CD36$^+$/Epo$^-$ EPCs expressed the B19V capsid, as well as B19V VP2-encoding mRNA (0.7% relative to the β-actin mRNA) and D1/A1-2-spliced mRNA (0.4% relative to the β-actin mRNA). These results were consistent with findings obtained from virus entry and DNA replication assays, which revealed that the virus genome copy (gc) number did not increase in purified CD36$^+$/Epo$^-$ EPCs in the absence of Epo, whereas the gc number increased by 2.5- and 13-fold in cells treated with Epo for 2 h and overnight, respectively (Fig. 3D). Control CD36$^+$/Epo$^+$ EPCs supported an approximately 93-fold increase of the entered B19V genome. Interestingly, viral entry was most dramatic in CD36$^+$/Epo$^+$ EPCs, with a 17-fold increase compared to that in the untreated CD36$^+$/Epo$^-$ EPCs and an approximately 5- to 8-fold increase compared to that in cells treated with Epo for 2 h or overnight (Fig. 3D). The cell surface marker profile for CD36$^+$/Epo$^-$ EPCs treated with Epo for 2 h and overnight was slightly shifted toward the profile for CD36$^+$/Epo$^+$ EPCs, especially with respect to levels of the CD34, CD41, and CD71 markers (Fig. 2A and B). These results indicate that Epo treatment facilitates differentiation of BFU-E progenitors to CFU-E progenitors, that the latter loses both the CD34 and CD41 markers (37), and that Epo treatment enhances B19V virus entry into infected cells.

Taken together, these results demonstrate that CD36$^+$/Epo$^-$ EPCs do not support replication of the B19V genome, although B19V entered these cells; Epo treatment led to an increase of B19V entry to these cells and, more importantly, activated B19V replication. The notion that Epo/EpoR signaling is likely essential for B19V replication is further supported by the fact that an increase in levels of phosphorylated Jak2 (pJak2) and phosphorylated EpoR (pEpoR) (markers of Epo treatment) (25) was observed in cells treated with Epo for 2 h and overnight, relative to the levels in cells not treated with Epo (Fig. 4). Thus, our results suggest that the Epo/EpoR signaling is likely essential for B19V replication.

Epo stimulation in CD36$^+$/Epo$^-$ EPCs after virus entry is sufficient to stimulate B19V replication. We next confirmed

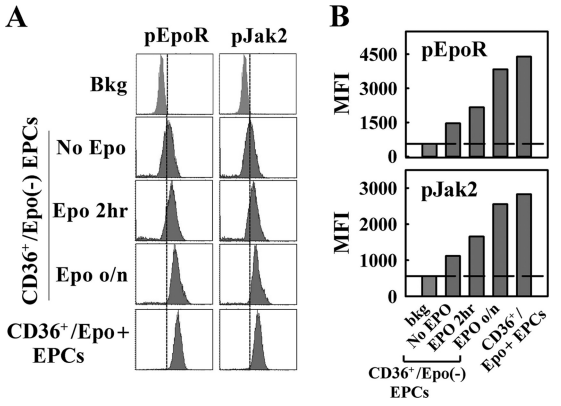

FIG. 4. An Epo pulse triggers EpoR signaling in CD36$^+$/Epo$^-$ EPCs. CD36$^+$/Epo$^-$ EPCs were pulsed with Epo (3 U/ml) for different lengths of time prior to B19V infection. Analysis was performed immediately after treatment and prior to B19V infection. CD36$^+$/Epo$^+$ EPCs expanded in Wong medium were used as controls. (A) For each treatment group, phosphorylation of EpoR and Jak2 prior to B19V infection was assessed by flow cytometry immediately before infection. Primary antibodies used were anti-pEpoR (Tyr 456) (Santa Cruz Biotechnology, Inc., Santa Cruz, CA), anti-pJak2 (Tyr 1007) (GenScript, Piscataway, NJ), and anti-B19V NS1 (12). (B) Quantification of data shown in panel A, with average mean fluorescence intensities (MFI) indicated by the bars and the background fluorescence indicated by the reference line. bkg, secondary antibody only.

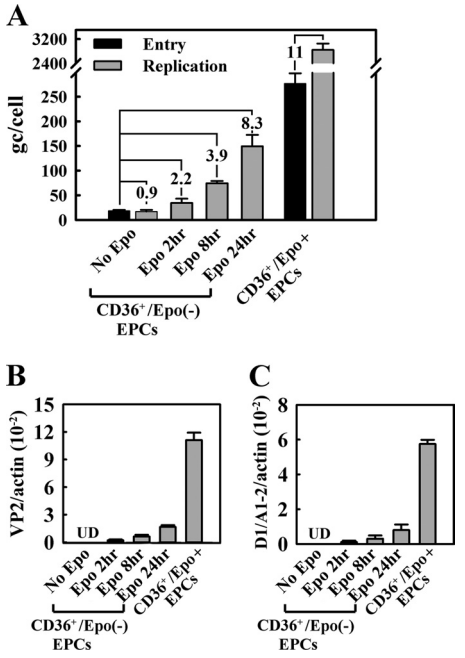

FIG. 5. An Epo pulse is critical for replication of the B19V genome in CD36$^+$/Epo$^-$ EPCs following virus entry. We recovered purified CD36$^+$/Epo$^-$ EPCs from StemCell medium for 1 h and then infected cells with B19V. One-fifth of the cells were used to quantify viral entry, and the other four-fifths were evenly divided into four groups treated with Epo for 0, 2, 8, and 24 h, respectively. Analysis was performed at 24 h p.i. CD36$^+$/Epo$^+$ EPCs expanded in Wong medium were used as controls. (A) B19V entry and replication were quantified by qPCR and are presented as the average numbers of B19V genome copies per cell (gc/cell). (B and C) The B19V VP2-encoding (B) and D1/A1-2-spliced (C) mRNAs were quantified by RT-qPCR and are presented as the average numbers of mRNA copies per β-actin mRNA (internal control). Standard deviations are shown in the panels and were calculated from at least three independent experiments. UD, undetectable.

the role of Epo in supporting B19V replication by performing a B19V entry assay prior to Epo stimulation. B19V replication was assayed at 24 h p.i. to minimize reinfection by progeny virus. Under these conditions, the numbers of viral genomes in the cells in different test groups were exactly the same at the time of Epo treatment. Again, CD36$^+$/Epo$^+$ EPCs were used as controls. Whereas no replication was observed at 24 h p.i. in the absence of Epo stimulation, replication in cells treated with Epo for 2, 8, and 24 h led to 2.2-, 3.9-, and 8.3-fold increases, respectively, in the viral genome copy numbers (Fig. 5A). Replication in the control CD36$^+$/Epo$^+$ EPCs led to an 11-fold increase in the number of viral genomes over the same period at 24 h p.i. In terms of B19V mRNA production, there was an absolute dependence on Epo; no VP2-encoding or D1/A1-2-spliced mRNAs were detected in infected cells in the absence of Epo (Fig. 5B and C). Increasing the length of the Epo treatment led to increasing levels of both the VP2-encoding and D1/A1-2-spliced mRNAs from infected CD36$^+$/Epo$^-$ EPCs, although the levels were still lower than those in the CD36$^+$/Epo$^+$ EPCs.

These results confirm that Epo plays a pivotal role in B19V replication, is absolutely required to activate replication of the B19V genome after virus entry to the cells, and confers permissiveness to B19V infection.

B19V replication in CD36$^+$/Epo$^+$ EPCs requires Jak2 phosphorylation. Epo ligation triggers EpoR dimerization and, in turn, phosphorylates EpoR-associated Jak2 (25). Phosphorylated Jak2 then phosphorylates tyrosine residues in the cytoplasmic tail of EpoR. We investigated whether this pJak2-mediated Epo/EpoR signaling facilitates B19V replication using AG490, a Jak2-specific inhibitor (27). The inhibitory effect of AG490, at 2 and 5 μM, was confirmed by Western blotting for pJak2 and pEpoR (Fig. 6A) and was found to be dose dependent. In the sample treated with 5 μM AG490, pJak2 and pEpoR were decreased to approximately 20% and 30%, respectively, of the level in the dimethyl sulfoxide (DMSO) controls. The cytotoxicity of AG490 in CD36$^+$/Epo$^+$ EPCs was monitored using the CellTiter-Glo kit obtained from Promega (Fig. 6B). No significant reduction of cell viability was observed at either concentration. Furthermore, AG490-treated cells did not show a significant level of cell death by annexin V/PI staining or that of cell cycle arrest by DAPI staining compared to those of their DMSO-treated counterparts (Fig. 6C). However, even at 2 μM AG490, B19V infection was significantly inhibited. B19V replication was reduced by 20-fold (Fig. 7A, compare lanes 3 and 2), and expression of both the B19V VP2-encoding and D1/A1-2-spliced mRNAs was reduced (Fig. 7B). Strikingly, when AG490 at 5 μM was used, both replication of the B19V DNA and expression of the VP2-encoding and D1/A1-2-spliced mRNAs were undetectable (Fig. 7A, lane 4, and Fig. 7B and C), indicating that B19V infection of CD36$^+$/Epo$^+$ EPCs is sensitive to AG490 treatment. Notably, AG490 treatment did not affect B19V entry to the cells (Fig. 7C).

To confirm the specificity of the requirement for Jak2 signaling in B19V replication, we tested the effects of Jak2 knock-

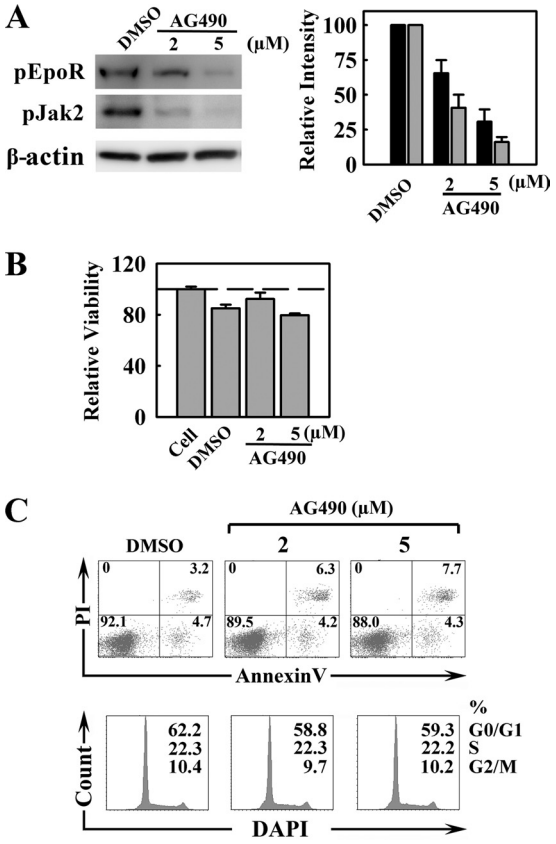

FIG. 6. Treatment of CD36$^+$/Epo$^+$ EPCs with the Jak2-specific inhibitor AG490 leads to a dose-dependent decrease in phosphorylated Jak2 and EpoR but does not affect the cell cycle. At day 7 in culture, CD36$^+$/Epo$^+$ EPCs were treated with AG490 at the indicated concentrations or with DMSO (0.5%; control). They were infected with B19V 24 h later (day 8). (A) Protein phosphorylation was assessed by Western blotting of a subpopulation of the cells using the indicated antibodies (left), and the bands were quantitated relative to their counterparts in DMSO (right). (B) Cell viability (to assess cytotoxicity of treatment), as evaluated using the CellTiter-Glo kit. The luminescence readings shown are normalized against values for the cell control group (no treatment). (C) Cell viability (to assess cytotoxicity of treatment), as evaluated by annexin V/PI staining (cell death) and DAPI staining (indicator of cell cycle stage). For annexin V/PI staining, the numbers shown in the lower left quadrants represent the percentages of live cells, and the numbers in each upper and lower right quadrants represent the percentages of later/early apoptotic cells. In the case of DAPI staining, the numbers represent the percentages of cells in each phase of the cell cycle (G_0/G_1, S, and G_2/M).

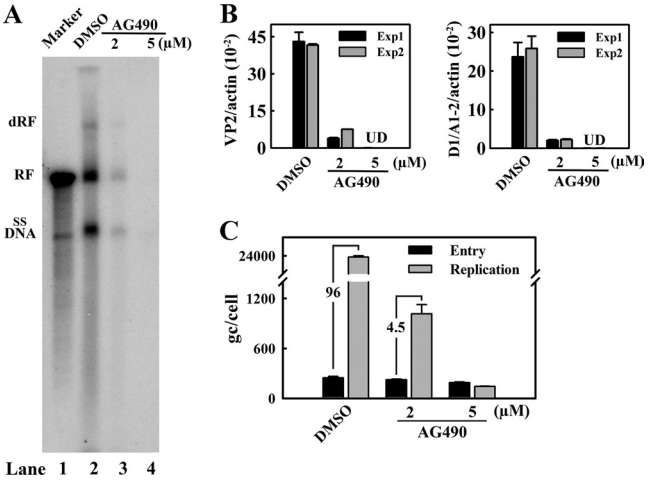

FIG. 7. Treatment with the Jak2-specific inhibitor AG490 abolishes B19V replication in CD36$^+$/Epo$^+$ EPCs. CD36$^+$/Epo$^+$ EPCs at day 7 were treated with AG490 at the indicated concentrations. They were infected with B19V 24 h later (day 8) and analyzed at 48 h p.i. (A) Hirt DNA was extracted from infected cells and analyzed by Southern blotting. The double replicative form (dRF), replicative form (RF), and single-stranded DNA form (ssDNA) of B19V are indicated. The 5.6-kb marker has been described previously (22). (B) Expression of VP2 and D1/A1-2-spliced mRNAs were quantified by RT-qPCR and are presented as the number of copies per β-actin mRNA (internal control). UD, undetectable; Exp, experiment. (C) B19V entry and replication were quantified by qPCR, as described in Materials and Methods, and are presented as the average numbers of B19V genome copies (gc) per cell. Standard deviations were calculated from at least three independent experiments.

down using a lentivirus expressing a Jak2-specifc shRNA (Lenti-GFP-Jak2-shRNA) and a control lentivirus expressing scrambled shRNA (Lenti-GFP-Scramble-shRNA). CD36$^+$/Epo$^+$ EPCs were pretreated with these lentiviruses 2 days prior to B19V infection. At 2 days p.i., GFP-expressing cells were gated and analyzed by flow cytometry using anti-Jak2 and anti-B19V NS1 antibodies. Consistent with the decrease in Jak2 levels, in GFP-Jak2-shRNA-expressing cells (with approximately 50% knockdown), the level of B19V NS1 detection was decreased by approximately 50%, relative to that in GFP-Scramble-shRNA-expressing cells (Fig. 8A). However, GFP-expressing cells did not show a significant level of cell death or cell cycle arrest compared with that of the GFP-negative cells (data not shown). Replication of the B19V genome, assessed based on levels of B19V VP2-encoding and D1/A1-2-spliced mRNAs, decreased by approximately 3-fold in Lenti-GFP-Jak2-shRNA-transduced cells (Fig. 8B and C), confirming the importance of Jak2 in B19V infection of CD36$^+$/Epo$^+$ EPCs. Overall, these results indicate that the Epo/EpoR/Jak2 signaling pathway is crucial to B19V infection of CD36$^+$/Epo$^+$ EPCs.

CD36$^+$/Epo$^-$ EPCs are permissive to B19V infection when EpoR is constitutively activated. To further corroborate the role of the Epo/EpoR/Jak2 signaling pathway during B19V infection, we generated a retroviral vector that expresses constitutively active EpoR (20). Purified CD36$^+$/Epo$^-$ EPCs were transduced with Retro-EpoR or Retro-GFP (as a control) 48 h prior to B19V infection. At 48 h p.i., GFP-expressing cells (approximately 50% of the total cell population) were gated and analyzed by flow cytometry, following intracellular staining with anti-pEpoR, anti-pJak2, and anti-B19V NS1 antibodies. Retro-EpoR-transduced cells expressed constitutively activated EpoR, as shown by an increase in the level of pEpoR (presumably phosphorylated by detected active pJak2), compared to that in Retro-GFP-transduced cells (Fig. 9A). The expression of constitutively active EpoR caused cells of the erythroid lineage to take on an expression profile typical of CD36$^+$/Epo$^+$ EPCs, including a decrease in the level of CD34 and an increase in the levels of GPA and CD71 (Fig. 9B).

Consistent with the observed change in the differentiation stage, the Retro-EpoR-transduced cells showed a significant increase in B19V NS1 expression (approximately 40% of the

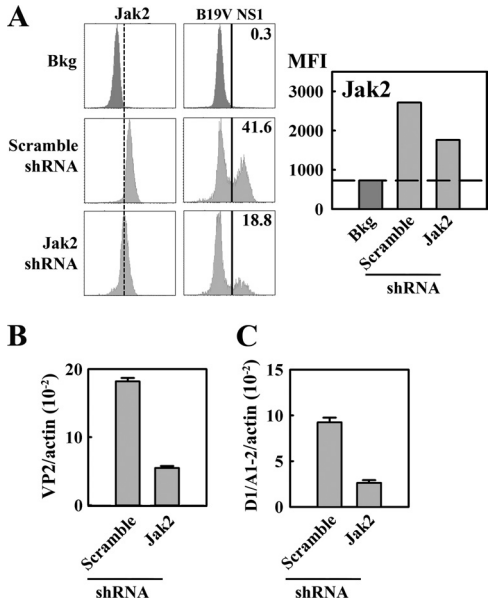

FIG. 8. CD36$^+$/Epo$^+$ EPCs treated with Jak2-specific shRNA show reduced susceptibility to B19V infection. CD36$^+$/Epo$^+$ EPCs at day 6 of culture were transduced with Lenti-GFP-Jak2-shRNA and Lenti-GFP-Scramble-shRNA. They were infected with B19V 48 h later (day 8) and analyzed at 48 h p.i. (A) Expression levels of Jak2 and B19V NS1 in GFP-expressing cells were selectively gated to quantify the expression levels of Jak2 and B19V NS1 by flow cytometry (left) and quantification thereof (right). Histograms indicate the average percentage of B19NS1-expressing cells in each group, and quantification is based on the MFI of Jak2 expression. Bkg, secondary antibody-only staining background. (B and C) Cells were harvested for mRNA isolation using the Turbo mRNA kit, as described in Materials and Methods. RT-qPCR was carried out to assess the B19V VP2-encoding mRNA/β-actin mRNA (B) and the B19V D1/A1-2-spliced mRNA/β-actin mRNA (C). Histograms illustrated in panels B and C show the averages and standard deviations and were calculated from at least three independent experiments.

cells) versus 1.1% of Retro-GFP-transduced cells (Fig. 9A). Levels of B19V mRNAs and replication of the B19V genome were also found to be significantly high in Retro-EpoR-transduced cells but not detectable in the Retro-GFP-transduced control cells (Fig. 9C and D). Consistent with the observations documented in Fig. 3D, B19V entry was increased by approximately 6.2-fold in Retro-EpoR-transduced cells compared to that in Retro-GFP-transduced cells; however, the B19V genome in these cells replicated by approximately 86-fold (Fig. 9C), suggesting that expression of constitutively active EpoR facilitates B19V entry into the cells and, more importantly, accommodates replication of these B19V genomes. These results are direct evidence that expression of constitutively active EpoR renders B19V-nonpermissive CD36$^+$/Epo$^-$ EPCs susceptible to B19V infection, confirming the role of the Epo/EpoR/Jak2 signaling pathway in B19V infection of erythroid progenitor cells.

B19V permissiveness of CD36$^+$/Epo$^+$ EPCs is sensitive to the concentration of Epo. We next sought to confirm that Epo plays a role in B19V infection of CD36$^+$/Epo$^+$ EPCs expanded in Wong medium. To this end, we cultured cells from day 4 stocks in Wong medium with a range of concentrations of Epo. These cells were infected at day 8 and analyzed at 48 h p.i. We found that as the Epo concentration rose from 0.1 to 0.5 and 2 U/ml, the percentage of NS1-expressing cells also increased (from 12% to 30% and 50%, respectively), as determined by flow cytometry using anti-NS1 antibody (Fig. 10A). No significant difference in NS1 expression between the groups treated with Epo at 2 and 10 U/ml was observed. Consequently, with this observation, the phosphorylation of both EpoR and Jak2 increased proportionally in the groups exposed to Epo at levels from 0.1 to 0.5 and 2 U/ml but was similar in the groups treated with 2 and 10 U/ml Epo (Fig. 10A). In addition, we observed an increase of B19V infection in these groups, as determined based on the levels of the B19V VP2-encoding and D1/A1-2-spliced mRNAs and the levels of B19V DNA replication (Fig. 10B and C). The levels of B19V entry into cells, in contrast, were found to be similar across all treatment groups (Fig. 10C), as well as those of cell survival and entered S-phase entry (Fig. 10D). Collectively, these experiments reveal that the level of B19V infection in CD36$^+$/Epo$^+$ EPCs is dependent on the Epo concentration, confirming that Epo plays an essential role in B19V replication.

DISCUSSION

In this study, we provide strong evidence that the Epo/EpoR/Jak2 signaling pathway is important for B19V replication in erythroid progenitor cells. Although a previous study had shown that Epo is essential for the differentiation of human hematopoietic stem cells into a population susceptible to B19V (52), the role of Epo in B19V infection was thought to be solely directing this differentiation specifically to BFU-E progenitors, CFU-E progenitors, and erythroblasts.

Effects of Epo on differentiation of erythroid progenitor cells. Erythropoiesis is a regulated process whereby hematopoietic progenitor cells give rise to committed erythroid progenitor cells, differentiate, and proliferate into mature red blood cells. This process involves an Epo-independent early phase, commitment of pluripotent hematopoietic stem cells to the erythroid lineage, and an Epo-dependent late phase during which these precursors mature into terminally differentiated, circulating enucleated erythrocytes. The commitment of hematopoietic stem cells to an erythroid progenitor (BFU-E and CFU-E) fate is independent of Epo expression (36, 40, 58, 59) and can be triggered by stem cell factor (SCF) (15, 33, 40, 59), interleukin-6 (IL-6) (51), and IL-3 (40). Epo acts late in erythropoiesis, is erythroid lineage specific, and supports the proliferation and maturation of committed erythroid progenitors (24, 36). Interestingly, Epo-independent erythrocyte production has also been reported (51).

We demonstrate that key markers of the erythroid progenitor fate, which are expressed on cells expanded in Wong medium (CD36$^+$/Epo$^+$ EPCs), define these cells as CFU-E-type progenitors on day 8, and their counterparts expanded in StemCell medium (CD36$^+$/Epo$^-$ EPCs) are defined as BFU-E-type progenitors, potentially at the verge of transitioning from the BFU-E to the CFU-E stage.

Effects of Epo on B19V infection of erythroid progenitor cells, implication for mechanism of virus entry, and a major role in virus genome replication. Our observation that CD36$^+$/Epo$^+$ EPCs expanded in Wong medium allow B19V to enter cells at a particularly high efficiency level (approximately 17

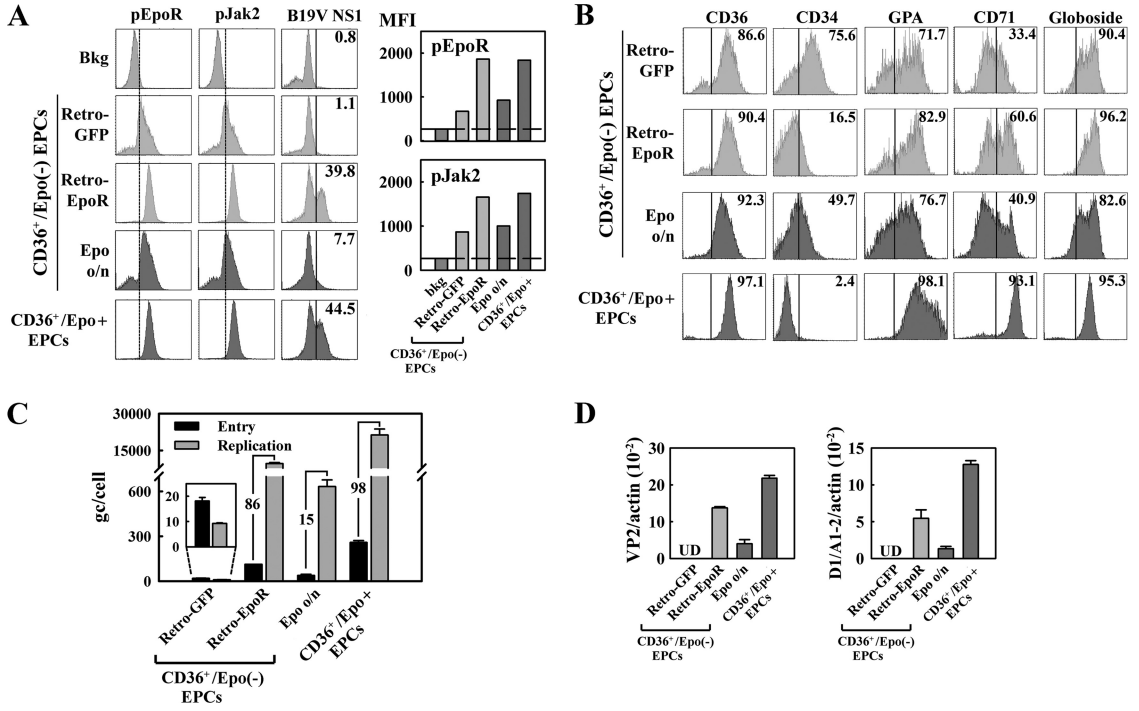

FIG. 9. CD36$^+$/Epo$^-$ EPCs transduced with constitutively active EpoR are permissive to B19V infection. Purified CD36$^+$/Epo$^-$ EPCs were transduced with GFP control retrovirus (Retro-GFP) and constitutively active EpoR-expressing retrovirus (Retro-EpoR). They were infected with B19V 48 h after retrovirus transduction. (A) At 48 h p.i., expression levels of pJak2, pEpoR, and B19V NS1 in GFP-expressing cells were assessed by flow cytometry (left). The MFI of pEpoR and pJak2 expression were quantified and are presented in the bar graphs (right). bkg, background staining with secondary antibody. (B) Expression of key cell surface markers of erythroid progenitors as indicated at 48 h p.t., prior to B19V infection. GFP-expressing cells of the Retro-GFP and Retro-EpoR groups were selectively gated. A representative result from two independent experiments is shown. (C) Levels of B19V entry and genome replication in cells of the indicated treatment groups were quantified by qPCR and are presented as the numbers of genome copies (gc) per cell. Fold differences between replication and virus entry are shown. The bars of the Retro-GFP group are enlarged to scale for better comparison. (D) Expression of B19V mRNAs at 48 h p.i. was assessed using RT-qPCR for the ratio of B19V VP2-encoding mRNA to β-actin mRNA and the ratio of B19V D1/A1-2-spliced mRNA to β-actin mRNA. UD, undetectable. Two groups of cells, CD36$^+$/Epo$^-$ EPCs treated with Epo overnight (Epo o/n) and CD36$^+$/Epo$^+$ EPCs, served as controls. Averages and standard deviations are shown in panels C and D and were calculated from at least three independent experiments.

times higher than that of the CD36$^+$/Epo$^-$ EPCs) was surprising. This could potentially be due to the observed increase in expression of the B19V coreceptor CD49e (55) or a consequence of the activities of as-yet-unidentified coreceptors. However, it is unlikely a consequence of KU80 binding as previously proposed (32), given that fewer than 5% of CD36$^+$/Epo$^+$ EPCs expressed KU80, yet more than 80% of these cells were infected by B19V (Fig. 1) (56). In addition, although a significantly high percentage of CD36$^+$/Epo$^-$ cells expressed KU80 (approximately 86%), the level of B19V entry into these cells was much lower than that into CD36$^+$/Epo$^+$ EPCs (Fig. 2D). All of these results question KU80 as a coreceptor for B19V infection. Clearly, the mechanism by which B19V enters cells warrants further investigation.

On day 8 of culture, CD36$^+$ EPCs expanded in StemCell and Wong media were at a similar stage along the erythropoiesis pathway, and B19V entered both types of CD36$^+$ EPCs, albeit at different levels. A major difference in the absence of Epo stimulation, however, was the failure of B19V genomes present in CD36$^+$/Epo$^-$ EPCs to replicate. In light of our previous finding that expression of adenovirus genes enables the B19V genome to replicate in B19V-nonpermisisve 293 cells (22), we hypothesize that the current results reflect a requirement for a unique nuclear microenvironment for B19V replication. We propose that such an environment is created in erythroid progenitor cells by the Epo/EpoR/Jak2 signaling pathway.

Key role of the Epo/EpoR/Jak2 pathway in B19V infection of erythroid progenitor cells. Jak2 plays a pivotal role in Epo signal transduction (34, 42). This kinase associates with EpoR at a membrane-proximal region of the cytoplasmic domain, where its binding to EpoR is thought to induce a conformational alteration of the EpoR cytoplasmic domain. This structural change in turn leads to the juxtaposition of Jak2 molecules in a manner conducive to transphosphorylation within the activation loop and, thus, to Jak2 activation. Upon activation, Jak2 phosphorylates 8 tyrosine residues in the EpoR cytoplasmic domain and autophosphorylates a number of additional sites (25). In addition, phosphorylated EpoR recruits and mediates the activation of SH2-binding factors (including STAT5, Grb2, and phosphatidylinositol 3-kinase [PI3K]) that signal though the Jak2/STAT5, Ras/MARK, and PI3K/AKT pathways. Activation of these pathways synergistically prevents apoptosis of committed erythroid progenitors, allowing them to undergo a predetermined program of terminal proliferation and erythroid differentiation. We have shown here that inhi-

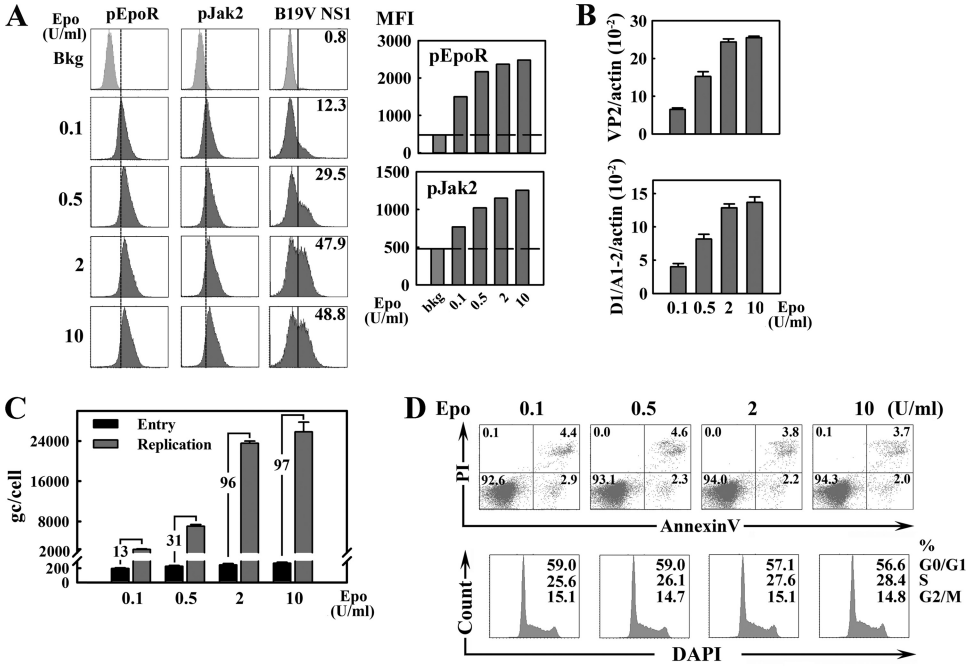

FIG. 10. B19V infection of $CD36^+/Epo^+$ EPCs is influenced by the Epo concentration in the culture medium. Day 4 stocks of $CD34^+$ HSCs expanded in Wong medium were cultured in Wong medium containing Epo at the indicated concentrations until day 8, when B19V infection was carried out. Infected cells were analyzed at 48 h p.i. (A) Epo pathway signaling in infected cells was assessed by flow cytometry for p-EpoR, pJak2, and B19V NS1 (left) and quantification using MFI for pEpoR and pJak2 staining (right). (B) RT-qPCR-based mRNA quantification for VP2-encoding and D1/A1-2-spliced mRNAs, normalized to the level of β-actin mRNA. (C) Virus entry and genome replication. B19V genome copy numbers are expressed as gc/cell. Levels of virus entry were determined as described in Materials and Methods, and fold differences between replication and virus entry are shown. Averages and standard deviations are shown in panels B and C and were calculated from at least three independent experiments. (D) Cell viability and cell cycle stage in $CD36^+/Epo^+$ EPCs expanded in Wong medium containing Epo at a concentration of 0.1, 0.5, 2, or 10 units/ml, as indicated, from days 4 through 8. Cells were then analyzed for cell death by annexin V/PI staining and cell cycle stage by DAPI staining. For annexin V/PI staining, the numbers shown in the lower left quadrants represent the percentages of live cells, and the numbers in upper and lower right quadrants represent the percentages of later/early apoptotic cells. In the case of DAPI staining, the numbers represent the percentages of cells in each phase of the cell cycle (G_0/G_1, S, and G_2/M).

bition of either Jak2 activity or EpoR phosphorylation abolishes B19V replication in infected erythroid progenitor cells. Together with the results obtained using the Jak2-specific shRNA, these results lead us to believe that Epo/EpoR/Jak2 signaling must be involved in B19V replication and provide a strong support for further investigation into the mechanisms underlying B19V replication in erythroid progenitors.

Previous studies have shown that expression of the constitutively active EpoR [the EpoR(R129C) mutant] can activate Jak2 in the absence of Epo binding (26). Our demonstration that Jak2 phosphorylation upon expression of this activated receptor in $CD36^+/Epo^-$ EPCs (Fig. 9A), and an accompanying increase in B19V infection, could be exacerbated by exposing cells to Epo at various concentrations (Fig. 10A) argues that the Epo/EpoR/Jak2 signaling pathway is critical to B19V infection. These conclusions are further supported by the fact that treating $CD36^+/Epo^-$ EPCs with Epo led to activation of B19V replication and to corresponding increases in the phosphorylation of both Jak2 and EpoR (Fig. 4). Collectively, our results strongly support the notion that signal transduction in response to EpoR activation involves the initial phosphorylation of Jak2, subsequent EpoR phosphorylation, and ultimately, B19V genome replication.

Interestingly, previous studies have indicated that that B19V can infect immortalized human microvascular endothelial cells and the human hepatocyte cell line HepG2 (18, 45), which might play a role in B19V infection-caused myocarditis (4, 6) and fulminant hepatitis (5, 23, 41, 48), respectively. EpoR is detectable on endothelial cells (35) and on hepatocytes (44), which may explain the B19V permissiveness of these cells under certain conditions.

In conclusion, our study provides evidence that Epo/EpoR/Jak2 signaling is essential for B19V replication and that EpoR activation either by Epo ligation or expression of constitutively active EpoR makes previously nonpermissive cells susceptible to B19V infection, activating replication of the B19V genome. It also indicates that Jak2-mediated phosphorylation of EpoR is necessary for this activation. This is a previously unappreciated role of Epo/EpoR/Jak2 signaling in supporting B19V infection and accounts for the unique tropism of B19V infection for human erythroid progenitors. In addition, our demonstration that AG490 abolishes B19V replication provides a potential starting point for the development of anti-B19V drugs.

ACKNOWLEDGMENTS

This work was supported by PHS grant R01 AI070723 from the NIAID and grant P20 RR016443 from the NCRR COBRE program.

We thank Murat O. Arcasoy at Duke University for the EpoR(R129C)-expressing construct.

REFERENCES

1. **Al-Khan, A., A. Caligiuri, and J. Apuzzio.** 2003. Parvovirus B-19 infection during pregnancy. Infect. Dis. Obstet. Gynecol. **11:**175–179.
2. **Anderson, M. J., M. N. Khousam, D. J. Maxwell, S. J. Gould, L. C. Happerfield, and W. J. Smith.** 1988. Human parvovirus B19 and hydrops fetalis. Lancet **i:**535.
3. **Asokan, A., J. B. Hamra, L. Govindasamy, M. Agbandje-McKenna, and R. J. Samulski.** 2006. Adeno-associated virus type 2 contains an integrin alpha5beta1 binding domain essential for viral cell entry. J. Virol. **80:**8961–8969.
4. **Basic, D., S. Gupta, and R. Y. Kwong.** 2010. Parvovirus b19-induced myocarditis mimicking acute myocardial infarction: clarification of diagnosis by cardiac magnetic resonance imaging. Circulation **121:**e40–e42.
5. **Bernuau, J., F. Durand, and D. Valla.** 1999. Parvovirus B19 infection and fulminant hepatitis. Lancet **353:**754–755.
6. **Bock, C. T., K. Klingel, and R. Kandolf.** 2010. Human parvovirus B19-associated myocarditis. N. Engl. J. Med. **362:**1248–1249.
7. **Bonvicini, F., C. Filippone, S. Delbarba, E. Manaresi, M. Zerbini, M. Musiani, and G. Gallinella.** 2006. Parvovirus B19 genome as a single, two-state replicative and transcriptional unit. Virology **347:**447–454.
8. **Brown, K. E., S. M. Anderson, and N. S. Young.** 1993. Erythrocyte P antigen: cellular receptor for B19 parvovirus. Science **262:**114–117.
9. **Brown, K. E., and N. Young.** 1997. Human parvovirus B19: pathogenesis of disease, p. 105–119. *In* L. J. Anderson and N. Young (ed.), Human parvovirus B19, vol. 20. Karger, Basel, Switzerland.
10. **Brown, K. E., N. S. Young, and J. M. Liu.** 1994. Molecular, cellular and clinical aspects of parvovirus B19 infection. Crit. Rev. Oncol. Hematol. **16:**1–31.
11. **Chen, A. Y., Y. Luo, F. Cheng, Y. Sun, and J. Qiu.** 2010. Bocavirus infection induces a mitochondrion-mediated apoptosis and cell cycle arrest at G_2/M phase. J. Virol. **84:**5615–5626.
12. **Chen, A. Y., E. Y. Zhang, W. Guan, F. Cheng, S. Kleiboeker, T. M. Yankee, and J. Qiu.** 2010. The small 11kDa non-structural protein of human parvovirus B19 plays a key role in inducing apoptosis during B19 virus infection of primary erythroid progenitor cells. Blood **115:**1070–1080.
13. **Chisaka, H., E. Morita, N. Yaegashi, and K. Sugamura.** 2003. Parvovirus B19 and the pathogenesis of anaemia. Rev. Med. Virol. **13:**347–359.
14. **Cotmore, S. F., and P. Tattersall.** 2005. Structure and organization of the viral genome, p. 73–94. *In* J. Kerr, S. F. Cotmore, M. E. Bloom, R. M. Linden, and C. R. Parrish (ed.), Parvoviruses. Hodder Arnold, London, United Kingdom.
15. **Dai, C. H., S. B. Krantz, and K. M. Zsebo.** 1991. Human burst-forming units-erythroid need direct interaction with stem cell factor for further development. Blood **78:**2493–2497.
16. **de Jong, E. P., T. R. de Haan, A. C. Kroes, M. F. Beersma, D. Oepkes, and F. J. Walther.** 2006. Parvovirus B19 infection in pregnancy. J. Clin. Virol. **36:**1–7.
17. **de Wolf, J. T., E. W. Muller, D. H. Hendriks, R. M. Halie, and E. Vellenga.** 1994. Mast cell growth factor modulates CD36 antigen expression on erythroid progenitors from human bone marrow and peripheral blood associated with ongoing differentiation. Blood **84:**59–64.
18. **Duechting, A., C. Tschope, H. Kaiser, T. Lamkemeyer, N. Tanaka, S. Aberle, F. Lang, J. Torresi, R. Kandolf, and C. T. Bock.** 2008. Human parvovirus B19 NS1 protein modulates inflammatory signaling by activation of STAT3/PIAS3 in human endothelial cells. J. Virol. **82:**7942–7952.
19. **Filippone, C., R. Franssila, A. Kumar, L. Saikko, P. E. Kovanen, M. Soderlund-Venermo, and K. Hedman.** 2010. Erythroid progenitor cells expanded from peripheral blood without mobilization or preselection: molecular characteristics and functional competence. PLoS One **5:**e9496.
20. **Fu, P., X. Jiang, and M. O. Arcasoy.** 2009. Constitutively active erythropoietin receptor expression in breast cancer cells promotes cellular proliferation and migration through a MAP-kinase dependent pathway. Biochem. Biophys. Res. Commun. **379:**696–701.
21. **Guan, W., F. Cheng, Y. Yoto, S. Kleiboeker, S. Wong, N. Zhi, D. J. Pintel, and J. Qiu.** 2008. Block to the production of full-length B19 virus transcripts by internal polyadenylation is overcome by replication of the viral genome. J. Virol. **82:**9951–9963.
22. **Guan, W., S. Wong, N. Zhi, and J. Qiu.** 2009. The genome of human parvovirus B19 virus can replicate in non-permissive cells with the help of adenovirus genes and produces infectious virus. J. Virol. **83:**9541–9553.
23. **Karetnyi, Y. V., P. R. Beck, R. S. Markin, A. N. Langnas, and S. J. Naides.** 1999. Human parvovirus B19 infection in acute fulminant liver failure. Arch. Virol. **144:**1713–1724.
24. **Koury, M. J., and M. C. Bondurant.** 1992. The molecular mechanism of erythropoietin action. Eur. J. Biochem. **210:**649–663.
25. **Lodish, H. F., S. Ghaffari, M. Socolovsky, W. Tong, and J. Zhang.** 2009. Intracellular signaling by the erythropoietin receptor, p. 155–174. *In* S. G. Elliott, M. A. Foote, and G. Molineux (ed.), Erythropoietins, erythropoietic factors and erythropoiesis. Birkhäuser Verlag, Basel, Switzerland.
26. **Longmore, G. D., and H. F. Lodish.** 1991. An activating mutation in the murine erythropoietin receptor induces erythroleukemia in mice: a cytokine receptor superfamily oncogene. Cell **67:**1089–1102.
27. **Meydan, N., T. Grunberger, H. Dadi, M. Shahar, E. Arpaia, Z. Lapidot, J. S. Leeder, M. Freedman, A. Cohen, A. Gazit, A. Levitzki, and C. M. Roifman.** 1996. Inhibition of acute lymphoblastic leukaemia by a Jak-2 inhibitor. Nature **379:**645–648.
28. **Miyagawa, E., T. Yoshida, H. Takahashi, K. Yamaguchi, T. Nagano, Y. Kiriyama, K. Okochi, and H. Sato.** 1999. Infection of the erythroid cell line, KU812Ep6 with human parvovirus B19 and its application to titration of B19 infectivity. J. Virol. Methods **83:**45–54.
29. **Moffatt, S., N. Yaegashi, K. Tada, N. Tanaka, and K. Sugamura.** 1998. Human parvovirus B19 nonstructural (NS1) protein induces apoptosis in erythroid lineage cells. J. Virol. **72:**3018–3028.
30. **Morey, A. L., and K. A. Fleming.** 1992. Immunophenotyping of fetal haemopoietic cells permissive for human parvovirus B19 replication in vitro. Br. J. Haematol. **82:**302–309.
31. **Morita, E., K. Tada, H. Chisaka, H. Asao, H. Sato, N. Yaegashi, and K. Sugamura.** 2001. Human parvovirus B19 induces cell cycle arrest at G(2) phase with accumulation of mitotic cyclins. J. Virol. **75:**7555–7563.
32. **Munakata, Y., T. Saito-Ito, K. Kumura-Ishii, J. Huang, T. Kodera, T. Ishii, Y. Hirabayashi, Y. Koyanagi, and T. Sasaki.** 2005. Ku80 autoantigen as a cellular coreceptor for human parvovirus B19 infection. Blood **106:**3449–3456.
33. **Muta, K., S. B. Krantz, M. C. Bondurant, and C. H. Dai.** 1995. Stem cell factor retards differentiation of normal human erythroid progenitor cells while stimulating proliferation. Blood **86:**572–580.
34. **Neubauer, H., A. Cumano, M. Muller, H. Wu, U. Huffstadt, and K. Pfeffer.** 1998. Jak2 deficiency defines an essential developmental checkpoint in definitive hematopoiesis. Cell **93:**397–409.
35. **Noguchi, C. T., L. Wang, H. M. Rogers, R. Teng, and Y. Jia.** 2008. Survival and proliferative roles of erythropoietin beyond the erythroid lineage. Expert Rev. Mol. Med. **10:**e36.
36. **Ogawa, M.** 1993. Differentiation and proliferation of hematopoietic stem cells. Blood **81:**2844–2853.
37. **Okumura, N., K. Tsuji, and T. Nakahata.** 1992. Changes in cell surface antigen expressions during proliferation and differentiation of human erythroid progenitors. Blood **80:**642–650.
38. **Ozawa, K., J. Ayub, Y. S. Hao, G. Kurtzman, T. Shimada, and N. Young.** 1987. Novel transcription map for the B19 (human) pathogenic parvovirus. J. Virol. **61:**2395–2406.
39. **Ozawa, K., G. Kurtzman, and N. Young.** 1986. Replication of the B19 parvovirus in human bone marrow cell cultures. Science **233:**883–886.
40. **Papayannopoulou, T., M. Brice, and C. A. Blau.** 1993. Kit ligand in synergy with interleukin-3 amplifies the erythropoietin-independent, globin-synthesizing progeny of normal human burst-forming units-erythroid in suspension cultures: physiologic implications. Blood **81:**299–310.
41. **Pardi, D. S., Y. Romero, L. E. Mertz, and D. D. Douglas.** 1998. Hepatitis-associated aplastic anemia and acute parvovirus B19 infection: a report of two cases and a review of the literature. Am. J. Gastroenterol. **93:**468–470.
42. **Parganas, E., D. Wang, D. Stravopodis, D. J. Topham, J. C. Marine, S. Teglund, E. F. Vanin, S. Bodner, O. R. Colamonici, J. M. van Deursen, G. Grosveld, and J. N. Ihle.** 1998. Jak2 is essential for signaling through a variety of cytokine receptors. Cell **93:**385–395.
43. **Pillet, S., G. N. Le, T. Hofer, F. NguyenKhac, M. Koken, J. T. Aubin, S. Fichelson, M. Gassmann, and F. Morinet.** 2004. Hypoxia enhances human B19 erythrovirus gene expression in primary erythroid cells. Virology **327:**1–7.
44. **Pinto, J. P., S. Ribeiro, H. Pontes, S. Thowfeequ, D. Tosh, F. Carvalho, and G. Porto.** 2008. Erythropoietin mediates hepcidin expression in hepatocytes through EPOR signaling and regulation of C/EBPalpha. Blood **111:**5727–5733.
45. **Poole, B. D., J. Zhou, A. Grote, A. Schiffenbauer, and S. J. Naides.** 2006. Apoptosis of liver-derived cells induced by parvovirus B19 nonstructural protein. J. Virol. **80:**4114–4121.
46. **Qiu, J., F. Cheng, and D. Pintel.** 2007. The abundant R2 mRNA generated by Aleutian mink disease parvovirus is tricistronic, encoding NS2, VP1, and VP2. J. Virol. **81:**6993–7000.
47. **Riipinen, A., E. Vaisanen, M. Nuutila, M. Sallmen, R. Karikoski, M. L. Lindbohm, K. Hedman, H. Taskinen, and M. Soderlund-Venermo.** 2008. Parvovirus b19 infection in fetal deaths. Clin. Infect. Dis. **47:**1519–1525.
48. **Sokal, E. M., M. Melchior, C. Cornu, A. T. Vandenbroucke, J. P. Buts, B. J. Cohen, and G. Burtonboy.** 1998. Acute parvovirus B19 infection associated with fulminant hepatitis of favourable prognosis in young children. Lancet **352:**1739–1741.
49. **Sol, N., J. J. Le, I. Vassias, J. M. Freyssinier, A. Thomas, A. F. Prigent, B. B. Rudkin, S. Fichelson, and F. Morinet.** 1999. Possible interactions between the NS-1 protein and tumor necrosis factor alpha pathways in erythroid cell apoptosis induced by human parvovirus B19. J. Virol. **73:**8762–8770.
50. **Srivastava, A., and L. Lu.** 1988. Replication of B19 parvovirus in highly enriched hematopoietic progenitor cells from normal human bone marrow. J. Virol. **62:**3059–3063.
51. **Sui, X., K. Tsuji, S. Tajima, R. Tanaka, K. Muraoka, Y. Ebihara, K. Ikebu-**

chi, K. Yasukawa, T. Taga, T. Kishimoto, and T. Nakahata. 1996. Erythropoietin-independent erythrocyte production: signals through gp130 and c-kit dramatically promote erythropoiesis from human $CD34^+$ cells. J. Exp. Med. **183:**837–845.

52. **Takahashi, T., K. Ozawa, K. Takahashi, S. Asano, and F. Takaku.** 1990. Susceptibility of human erythropoietic cells to B19 parvovirus in vitro increases with differentiation. Blood **75:**603–610.
53. **Vainchenker, W., J. F. Deschamps, J. M. Bastin, J. Guichard, M. Titeux, J. Breton-Gorius, and A. J. McMichael.** 1982. Two monoclonal antiplatelet antibodies as markers of human megakaryocyte maturation: immunofluorescent staining and platelet peroxidase detection in megakaryocyte colonies and in in vivo cells from normal and leukemic patients. Blood **59:**514–521.
54. **Weigel-Kelley, K. A., M. C. Yoder, and A. Srivastava.** 2001. Recombinant human parvovirus B19 vectors: erythrocyte P antigen is necessary but not sufficient for successful transduction of human hematopoietic cells. J. Virol. **75:**4110–4116.
55. **Weigel-Kelley, K. A., M. C. Yoder, and A. Srivastava.** 2003. Alpha5beta1 integrin as a cellular coreceptor for human parvovirus B19: requirement of functional activation of beta1 integrin for viral entry. Blood **102:**3927–3933.
56. **Wong, S., N. Zhi, C. Filippone, K. Keyvanfar, S. Kajigaya, K. E. Brown, and N. S. Young.** 2008. Ex vivo-generated $CD36^+$ erythroid progenitors are highly permissive to human parvovirus B19 replication. J. Virol. **82:**2470–2476.
57. **Woolf, A. D., G. V. Campion, A. Chishick, S. Wise, B. J. Cohen, P. T. Klouda, O. Caul, and P. A. Dieppe.** 1989. Clinical manifestations of human parvovirus B19 in adults. Arch. Intern. Med. **149:**1153–1156.
58. **Wu, H., U. Klingmuller, P. Besmer, and H. F. Lodish.** 1995. Interaction of the erythropoietin and stem-cell-factor receptors. Nature **377:**242–246.
59. **Wu, H., X. Liu, R. Jaenisch, and H. F. Lodish.** 1995. Generation of committed erythroid BFU-E and CFU-E progenitors does not require erythropoietin or the erythropoietin receptor. Cell **83:**59–67.
60. **Yaegashi, N., T. Niinuma, H. Chisaka, S. Uehara, S. Moffatt, K. Tada, M. Iwabuchi, Y. Matsunaga, M. Nakayama, C. Yutani, Y. Osamura, E. Hirayama, K. Okamura, K. Sugamura, and A. Yajima.** 1999. Parvovirus B19 infection induces apoptosis of erythroid cells in vitro and in vivo. J. Infect. **39:**68–76.
61. **Yoto, Y., J. Qiu, and D. J. Pintel.** 2006. Identification and characterization of two internal cleavage and polyadenylation sites of parvovirus B19 RNA. J. Virol. **80:**1604–1609.
62. **Young, N. S., and K. E. Brown.** 2004. Parvovirus B19. N. Engl. J. Med. **350:**586–597.
63. **Zandstra, P. W., E. Conneally, A. L. Petzer, J. M. Piret, and C. J. Eaves.** 1997. Cytokine manipulation of primitive human hematopoietic cell self-renewal. Proc. Natl. Acad. Sci. U. S. A. **94:**4698–4703.
64. **Zhang, C. C., and H. F. Lodish.** 2008. Cytokines regulating hematopoietic stem cell function. Curr. Opin. Hematol. **15:**307–311.